EDGE ARTICLE

Check for updates

On 1,3-phosphaazaallenes and their diverse reactivity†

Malte Fischer [ID] and Christian Hering-Junghans [ID] *

1,3-Phosphaazaallenes are heteroallenes of the type RP=C=NR′ and little is known about their reactivity. In here we describe the straightforward synthesis of ArPCNR (Ar = Mes*, 2,4,6-*t*Bu-C$_6$H$_2$; ^{Mes}Ter, 2.6-(2,4,6-Me$_3$C$_6$H$_2$)–C$_6$H$_3$; ^{Dip}Ter, 2.6-(2,6-*i*Pr$_2$C$_6$H$_3$)–C$_6$H$_3$; R = *t*Bu; Xyl, 2,6-Me$_2$C$_6$H$_3$) starting from phospha-Wittig reagents ArPPMe$_3$ and isonitriles CNR. It is further shown that ArPCN*t*Bu are thermally labile with respect to the loss of iso-butene and it is shown that the cyanophosphines ArP(H)CN are synthetically feasible and form the corresponding phosphanitrilium borates with B(C$_6$F$_5$)$_3$, whereas deprotonation of ^{Dip}TerP(H)CN was shown to give an isolable cyanidophosphide. Lastly, the reactivity of ArPCNR towards Pier's borane was investigated, showing hydroboration of the C=N bond in Mes*PCN*t*Bu to give a hetero-butadiene, while with ^{Dip}TerPCNXyl the formation of the Lewis acid–base adduct with a B–P linkage was observed.

Introduction

1,3-Phosphaazaallenes (RP=C=NR) are a heteroallene subclass. The first derivative *t*BuPCN*t*Bu was obtained by combining *t*BuP(SiMe$_3$)C(OSiMe$_3$)=N*t*Bu with NaOH under the release of hexamethyldisiloxane.[1,2] Although known for almost 40 years, 1,3-phosphaazaallenes have been scarcely investigated, especially when compared to the "lighter" carbodiimides and other heteroallene analogues. Another synthetic route was disclosed by Yoshifuji,[3,4] and Appel,[5] who reacted Mes*P(Li)SiMe$_2$*t*Bu (Mes* = 2,4,6-*t*Bu$_3$C$_6$H$_2$) with isocyanates in a Peterson-type reaction to give Mes*PCNR (R = Ph, *n*Pr, *t*Bu). In 2000, Zhou and co-workers expanded this series to include Mes*PCN(4-ClC$_6$H$_4$).[6] Mes*PCN(4-ClC$_6$H$_4$) and Mes*PCNPh[4] are the only structurally characterized 1,3-phosphaazaallenes bearing classic organic substituents. Sterically demanding groups on the P atom suppress dimerization to the corresponding 1,3-diphosphetanes, which can only be reconverted to the 1,3-phosphaazaallenes by flash vacuum pyrolysis.[2,7] Even Mes*PCNPh slowly dimerizes in solution, whereas in the presence of catalytic amounts of Pd(PPh$_3$)$_4$ the unsymmetric four-membered heterocycle is obtained.[8] Derivatives with a bulky cyclopropen-1-yl substituent at the phosphorus were synthesized by Regitz *et al.*[9]

Leibniz Institut für Katalyse e.V. (LIKAT), A.-Einstein-Str. 3a, 18059 Rostock, Germany. E-mail: christian.hering-junghans@catalysis.de; Web: [https://www.catalysis.de/forschung/aktivierung-kleiner-molekuele/]

† Electronic supplementary information (ESI) available: Synthesis and characterization of compounds, NMR spectra, crystallographic, and computational details. CCDC 2086496–2086506. For ESI and crystallographic data in CIF or other electronic format see DOI: 10.1039/d1sc02947a

In 1991 Grobe and co-workers demonstrated that the meta-stable (F$_3$C)PCN*t*Bu (can be handled at −40 °C) is feasible by reacting the phosphaalkene precursor (F$_3$C)P=CF$_2$ with three equivalents of H$_2$N*t*Bu.[10] Instead of dimerizing at higher temperatures, (F$_3$C)PCN*t*Bu decomposes to give fluorinated cyclophosphanes (PCF$_3$)$_n$ and the isocyanide CN*t*Bu. Stephan *et al.* showed that the zirconocene phosphinidene Cp$_2$(PMe$_3$)Zr=PMes* reacts with an isothiocyanate in a [2 + 2] cycloaddition/cycloreversion sequence to yield Mes*PCNPh and [Cp$_2$ZrS]$_2$.[11] That 1,3-phosphaazaallenes can function as ligands for transition metals was established by Streubel and Jones.[12] Photochemical ring opening in the presence of an isocyanide of a W(CO)$_5$-stabilized 2*H*-azaphosphirene resulted in the formation of an 1,3-phosphaazaallene with the P atom remaining coordinated to W(CO)$_5$. A transient terminal phosphinidene complex is assumed to react in a 1,1-addition with the respective isocyanide. The motif to generate 1,3-phosphaazaallenes directly in the coordination sphere of a transition metal by reactions of metal-bound phosphinidenes with isocyanides is more common in the literature.[13] A trimethylstannyl substitution at the phosphorus centre in 1,3-phosphaazaallenes was achieved by reacting the potassium 1,3-azaphosphaallenide K[*i*PrNCP] with ClSnMe$_3$ in a salt metathesis reaction, thus revealing another access to this substance class.[14] The most recent examples of 1,3-phosphaazaallenes were synthesized by Bertrand *et al.* in coupling reactions of (phosphino)phosphinidenes with isocyanides.[15] Moreover, Scheschkewitz *et al.* showed that a phosphasilene with a mobile NMe$_2$-functionality on the phosphorus atom undergoes an NMe$_2$-shift in the reaction with CN*t*Bu to give a P-silyl-substituted 1,3-phosphaazaallene.[16] The synthetic protocols towards 1,3-phosphaazaallenes are summarized in Scheme 1. Even though

Scheme 1 Syntheses of 1,3-phosphaazaallenes and scope of this work.

Scheme 2 Reactions of **1a–c** with isocyanides to give 1,3-phosphaazaallenes **3a–f**; [a] obtained as a mixture with the diphosphenes Mes*PPMes* and ^{Mes}TerPP^{Mes}Ter, respectively; [b] heated to 60° (**3a**) or 80 °C (**3f**).

1,3-phosphaazaallenes are without a doubt an interesting class of compounds, it is surprising that their general reactivity has not been studied in detail.

Recently, we have revisited the chemistry of phosphanylidene phosphoranes, so-called phospha-Wittig reagents, ArPPMe$_3$ (**1a–c**) (**1a**: Ar = Mes*; **1b**: Ar = 2,6-(2,4,6-Me$_3$C$_6$H$_2$)–C$_6$H$_3$, ^{Mes}Ter, **1c**: Ar = 2.6-(2,6-iPr$_2$C$_6$H$_3$)–C$_6$H$_3$, ^{Dip}Ter).[17] We successfully used them as phosphinidene transfer reagents in reactions with N-heterocyclic carbenes (NHCs) or N-heterocyclic olefins (NHOs),[17] towards Al(ı) species to give phosphaalumenes,[18] and with Cp$_2$Ti(C$_2$(SiMe$_3$)$_2$) to afford terminal titanium phosphinidene complexes, respectively.[19] In this contribution, the reactivity of the phospha-Wittig reagents **1a–c** towards isocyanides is presented (Scheme 1, bottom), giving a series of 1,3-phosphaazaallenes. The tBu-substituted 1,3-phosphaazaallenes can be converted into primary cyanophosphines, which in one case can be transformed to the corresponding cyanophosphides. Finally, the reactivity of 1,3-phosphaazaallenes and primary cyanophosphines towards the perfluorinated arylboranes RB(C$_6$F$_5$)$_2$ (R = H, C$_6$F$_5$) is illustrated.

Results and discussion

In a first series of experiments Mes*PPMe$_3$ (**1a**)[14] was dissolved in C$_6$D$_6$, and an excess of CNtBu (**2a**) was added (Scheme 2).[20] Within 16 h at room temperature, two new signals were observed in the ^{31}P{^{1}H} NMR spectrum at −62.6 and −103.8 ppm, respectively, along with mostly unreacted starting materials. Heating to 60 °C for 24 h resulted in the consumption of **1a** and one equivalent of CNtBu to give the targeted 1,3-phosphaazaallene Mes*PCNtBu (**3a**, δ^{31}P{^{1}H} = −103.8 ppm) upon PMe$_3$ release. This is in contrast to the reaction of the phosphaketene [sP]PCO ([sP] = (H$_2$CNDip)$_2$P) with CN–Ad (Ad = adamantyl), which did not result in a CO for isonitrile

substitution, but in the formation of a P$_2$C$_2$ heterocycle through attack of CN–Ad on the PCO carbon atom.[21] However, sequential treatment of [sP]PCO with PPh$_3$ and CNAd was shown to afford the corresponding heteroallenes [sP]PCNAd.[22] Phosphaketenes are related to the 1,3-phosphaazaallenes through isolobal CO for CNR replacement.[23] To further investigate the scope of this reaction, **1a–c** were each reacted with both **2a** and CNXyl (Xyl = 2,6-Me$_2$C$_6$H$_3$, **2b**) (Scheme 2). It was found that the desired 1,3-phosphaazaallene formation is generally faster at higher temperatures but accompanied by diphosphene ArP=PAr formation unless ^{Dip}TerPPMe$_3$ (**1c**) is used. It is worthy to note that **3b** and **3d** could only be obtained as mixtures with the corresponding diphosphenes ^{Mes}TerP=P^{Mes}Ter,[24] and Mes*P=PMes*,[25] respectively, even if an excess of isocyanide was employed (Fig. S8 and S18†). Theoretical investigations at the PBE0-D3/def2SVP//DNLPO-CCSD(T)/def2TZVP level of theory revealed that the formation of **3a–f** are exergonic (Fig. S86†).[26,27] However, diphosphene formation from ArPPMe$_3$ through recombination of ArP upon PMe$_3$ release, has been calculated to be even more exergonic at the same level of theory, therefore explaining that formation of diphosphenes cannot be completely suppressed (Fig. S18†). Using a thermal approach, a diphosphene–poly(phenylenevinylene) has been prepared from the corresponding phospha-Wittig monomers upon PMe$_3$ release. The monomer showed the same 2,6-Mes$_2$Ar structural motif as in phospha-Wittig reagent **1b**.[28] In case of **1a** free phosphinidenes are unlikely, as cyclometalated species are not

Table 1 Characteristic ^{31}P{^{1}H} and ^{13}C{^{1}H} NMR data of **3a–f**. Calculated ^{31}P NMR shifts (PBE0-D3/def2SVP) are given in parentheses

Compound	δ^{31}P{^{1}H}^{a} (δ_{calc} ^{31}P)^a	δ^{13}C{^{1}H}(PCN)^a	$^1J_{P,C}$(PCN)^a
3a	−103.9 (−124.4)	192.2	76.8
3b	−125.4 (−161.1)	186.6	73.0
3c	−134.8 (−164.8)	177.9	77.9
3d	−120.6 (−157.9)	191.5	78.8
3e	−145.4 (−179.4)	183.7	78.1
3f	−144.8 (−164.1)	179.6	77.2

^{a} In C$_6$D$_6$ at room temperature; values given in ppm (δ) or Hz (J).

observed.[29] The NMR data of **3a–f** are in accordance to the previously reported data of **3a** in CDCl$_3$ (Table 1).[4] The ^{31}P{^{1}H} NMR signals of **3a–3f** range from −103.9 to −145.4 ppm and are generally shifted to higher field when the N-substituent is aromatic with the P-substituent being the same. This was corroborated by DFT calculations at the PBE0-D3/def2SVP level of theory, which gave $\delta_{calc}(^{31}P)$ values that are systematically at lower ppm values, though the experimentally observed trends are followed (Table 1).

Highly characteristic for **3a–f** are the ^{13}C{^{1}H}NMR signals of the two-coordinate carbon atoms of the PCN moieties, being significantly deshielded ($\delta^{13}C\{^1H\}$ = 177.9 to 192.2 ppm) and showing $^1J_{P,C}$ coupling constants of 73.0 to 78.1 Hz (Table 1). Additionally, the molecular structures of **3a**, **3e**, and **3f** could be determined by single crystal X-ray diffraction (SC-XRD, Fig. 1, Table 2). The P–C bond lengths of **3a**, **3e**, and **3f** of 1.6658(15) Å (**3a**) to 1.6785(12) Å (**3f**) are slightly elongated compared to **I** (1.651 Å) and **II** (1.642(5) Å), respectively, but are shorter than the sum of the covalent double bond radii (Σr_{cov}(P=C) = 1.69 Å).[30] The N–C bond lengths of **3a**, **3e**, and **3f** (1.2009(15) Å to 1.2037(19) Å) are in the expected range for heteroallenes (*cf.* XylN=C=NXyl d(C–N) 1.197(2), 1.206(3) Å).[31,32] Noteworthy, the P–C–N angles deviate from linearity (as expected for sp-hybridized carbon atoms) but are in good agreement to previously structurally characterized 1,3-phosphaazaallenes (Table 2).

The bonding in **3a–f** was studied using the truncated model compound MesPCNMe on the PBE0-D3/def2SVP level of theory. Inspection of the Kohn–Sham orbitals revealed a HOMO best described as a polarized P–C π-bond, while the LUMO shows major contribution from the C–N π* orbital interacting with a s-type lone pair on phosphorus (Fig. 2, top). With an energetically high lying HOMO the 1,3-phosphaazaallenes might be potentially oxidized to give the corresponding radical cation, as was recently shown for vinyl-substituted diphosphenes.[33] CV studies on **3a** show an irreversible oxidation event at $E_{1/2}$ = 0.38 V *vs.* Fc/ Fc$^+$ (Fig. S82–S84†), and the corresponding radical cation might be synthetically feasible. We next evaluated the NPA (Natural Population Analysis) charges indicating a minimal charge transfer from the MesP-fragment to the CNMe moiety by −0.196e, with a positive partial charge on P of 0.37e and 0.07e

on the two-coordinate C atom. Natural Bond Orbital (NBO) analysis supports the description as an heteroallene, with a LP of electrons on P and polarized σ- and π-P=CNMe (WBI 1.64) and PC≡NMe (WBI 2.05) double bonds, respectively. In agreement with the KS-orbitals the π-component is polarized towards the P atom (58.3% P, 41.7% C), whereas the σ-component is inversely polarized (34.5% P, 65.5% C). Analysis of the second order perturbation of the Fock matrix revealed delocalization of the lone pair of electrons (LP) on P into the CN π*-orbital resulting in a stabilization energy of 12.7 kcal mol^{-1}. Natural resonance theory analysis (NRT) revealed two leading resonance structures, with the 1,3-phosphaazaallene being the dominant form (31.7%) and an ylidic formulation with a C≡N triple bond and thus two LPs on P (14.8%) (Fig. 2, bottom).

Formation of cyanophosphines starting from 3a–c

When a solution of **3a** was heated to 105 °C in toluene-d_8 a new species with a ^{31}P{^{1}H} NMR chemical shift of −105.6 ppm (*cf.* **3a** δ^{31}P{^{1}H} = −103.9 ppm) was observed along with minimal amounts of the diphosphene Mes*P=PMes* (δ^{31}P{^{1}H} = 493.2 ppm). This transformation is accompanied by the formation of iso-butene, as evident from two signals in the ^{1}H NMR spectrum in a 3 : 1 ratio at 1.60 (triplet) and 4.75 (heptet) ppm, respectively. Finally, the multinuclear and multidimensional NMR data clearly showed that the new compound is the cyanophosphine Mes*P(H)CN (**4a**) (Scheme 3). Isobutene elimination and formal HCN transfer has been previously observed with dis-ilynes,[34] whereas with boracummulenes and transient borylenes CN$^-$ transfer was observed, with formation of a mixture of iso-butane and -butene.[35,36] Streubel and co-workers showed that the η^1-1,3-phosphaazaallene complex (Me$_3$Si)$_2$HC–P(W(CO)$_5$) CNtBu undergoes thermal loss of iso-butene to give the corresponding cyanophosphine tungsten complex.[12] The thermodynamic feasibility of this transformation was elucidated at the PBE0-D3/def2SVP//DNLPO-CCSD(T)/def2TZVP level of theory, showing that the formation of **4a** is exergonic by −36.93 kJ mol^{-1}, whereas the dimerization of **3a** to give Mes*P=PMes* and CNtBu is less favored ($\Delta_R G$ = −5.68 kJ mol^{-1}). A scan of the potential energy surface revealed that the H-shift from the tBu-group to P occurs intramolecularly
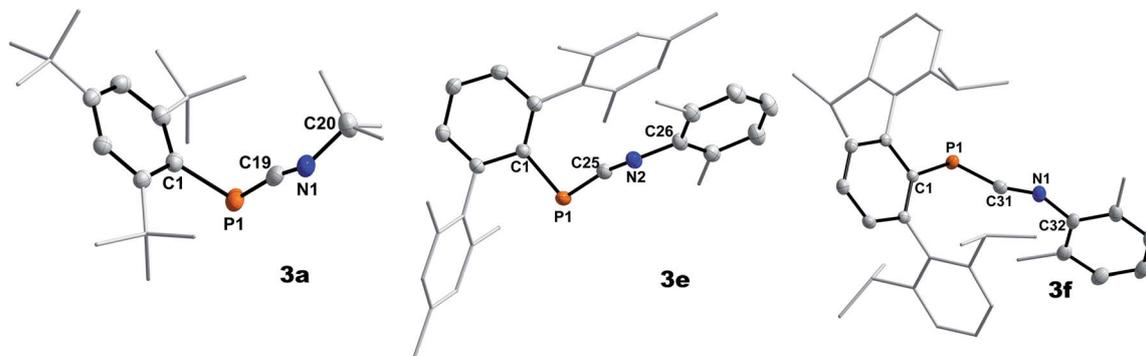

Fig. 1 Molecular structures of **3a** (left), **3e** (middle), and **3f** (right). Hydrogen omitted and parts of the molecule rendered as wireframe for clarity. Thermal ellipsoids are drawn at the 50% probability level. Structural parameters are summarized in Table 2.

Table 2 Selected bond lengths [Å] and angles [°] of **3a**, **3e** and **3f** (literature known species I and II for comparison)

Compound	P–C	N–C	P–C–N	C–P–C	C–N–C
3a	1.6690(15)	1.2034(18)	170.38(12)	97.92(6)	130.02(13)
3e	1.6658(15)	1.2037(19)	167.14(13)	103.06(7)	139.44(15)
3f	1.6785(12)	1.2009(15)	160.00(10)	107.53(5)	143.24(12)
Mes*PCNPh (**I**)[4]	1.651	1.209	171.1	99.2	130.5
Mes*PCN(p-ClC6H4) (**II**)[6]	1.642(5)	1.214(6)	170.8(4)	99.8(2)	128.3(4)

via a six-membered transition state ($\Delta_{\#}G = 156.1$ kJ mol^{-1}), resulting in P–H bond formation as the C(sp^3)–H and N–C$_{tBu}$ bonds are cleaved (Fig. S87†). This rather high energy barrier is in line with prolonged heating of the reaction mixture at 105 °C. An alternative radical pathway through N–C$_{tBu}$ bond homolysis and formation of a *t*Bu· radical was excluded as this would result in disproportionation and a mixture of iso-butene and iso-butane. The intermediate formation of free phosphinidenes is also unlikely, as this would give rise to cyclo-metalated species in case of Mes* and ^{Dip}Ter, which were not observed by NMR spectroscopy. Alternatively, **4a** can be prepared directly in one pot starting from **1a** and **2a** (Scheme 3, bottom).[16] Following this route **4a** was isolated as a colourless solid in good yields of 75%. Given the PH functionality, the ^{1}H NMR spectrum shows a characteristic doublet at 5.57 ppm with a $^1J_{P,H}$ coupling constant of 252.3 Hz, which is corroborated by the ^{31}P NMR spectrum. To further elaborate the scope of this reaction, the

analogous ^{Mes}TerP(H)CN (**4b**) and ^{Dip}TerP(H)CN (**4c**) derivatives were synthesized, and their characteristic NMR data is shown in Table 3. Surprisingly, in the IR spectrum of **4a** and **4c** no characteristic CN band is detected, in agreement with frequency analyses at the PBE0-D3/def2SVP level of theory. The presence of a P–H moiety was corroborated by a band at 2411 and 2310 cm^{-1} for **4a** and **4c**, respectively. Cyanophosphines of the general type RP(H)CN (R = alkyl, aryl) have long remained elusive and were either found to be unstable,[37] or to be stabilized by coordination to a transition metal.[38]

In 2001 the reaction of dicyanophosphines (RP(CN)$_2$) with equimolar amounts of Schwartz's reagent ([Cp$_2$Zr(H)Cl]$_n$) was shown to afford the methyl, *tert*-butyl, and Mes* derivatives, respectively.[39] However, structural data of this compound class is missing in the literature and the molecular structures of **4a–c** could be determined by SC-XRD (Fig. 3, Table 4). The C–N bond lengths in **4a–c** average 1.146 Å and indicate triple bonds ($\Sigma r_{cov}(C \equiv N) = 1.14$ Å),[30] in agreement with the formulation as cyanophosphines. The average P–C bond length of 1.791 Å is shorter than the respective single bond covalent radii ($\Sigma r_{cov}(P–C) = 1.86$ Å),[30] with a nearly linear arrangement of the P–C–N unit (>176°). Similar bond lengths were reported for Mes*P(CN)$_2$ (P–C$_{avg}$ 1.80 Å, N–C$_{avg}$ 1.14 Å).[39] NBO analyses of **4a–c** at the PBE0-D3/def2SVP//PBE0/def2SVP level of theory support the notation as cyanophosphines with CN triple bonds (WBI C$\equiv$N **4a** 2.88, **4b** 2.87, **4c** 2.87), a polar P$^{\delta+}$–C$^{\delta-}_{CN}$ single bond and a LP on P, which is minimally delocalized into two π* orbitals of the CN group with a stabilization energy of *ca.* 12 kcal mol^{-1}.[17]
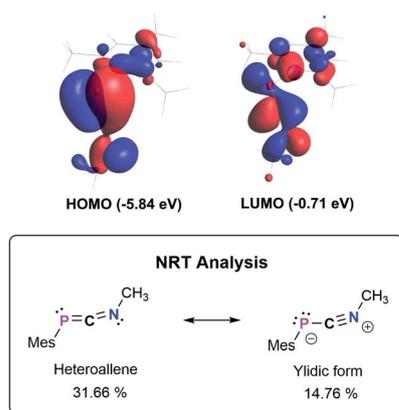
Fig. 2 Selected Kohn–Sham orbitals of the truncated model compound MesPCNMe (PBE0-D3/def2SVP) and leading resonance structures according to NRT analysis.

Reactivity of cyanophosphines towards B(C$_6$F$_5$)$_3$

4a–c possess two potential binding sites for Lewis acids, the LPs on P and N, even though steric congestion should render the phosphorus rather inaccessible. By reacting **4a–c** with B(C$_6$F$_5$)$_3$, the first examples of the corresponding phosphanitrilium borates RP(H)CNB(C$_6$F$_5$)$_3$ (R = Mes* (**5a**), R = ^{Mes}Ter (**5b**), R = ^{Dip}Ter (**5c**)) were prepared (Scheme 4). The reactions were performed on NMR scale and **5a** was exemplarily isolated as a colourless solid in a moderate yield of 55%. The coordination to the borane moiety results in a minimal deshielding of the PH unit accompanied by a slight increase of the $^1J_{P,H}$ coupling constant in both the ^{1}H and ^{31}P NMR spectra ($\delta(^1H) = 5.61$ ppm, $\delta(^{31}P) = -99.2$ ppm, $^1J_{P,H} = 260.0$ Hz; $\delta_{calc}(^{31}P) = -140.9$ ppm), respectively, when compared to the starting material **4a** ($\delta(^1H) = 5.57$ ppm, $\delta(^{31}P) = -105.4$ ppm, $^1J_{P,H} = 252.3$ Hz). The signals of the C$\equiv$N group are unaltered (**5a**: $\delta(^{13}C\{^1H\}) = 121.0$ ppm, *c.f.* **4a**: $\delta^{13}C\{^1H\} = 120.8$ Hz), while the $^1J_{P,C}$ coupling constant

Scheme 3 Formation of the cyanophosphines **4a–c** from **3a–c** (top) or directly from **1a–c** and *t*BuNC (**2a**).

Table 3 Characteristic $^{31}P\{^1H\}5.61$ and $^{13}C\{^1H\}$ NMR data of **4a–c**. Calculated ^{31}P NMR shifts (PBE0-D3/def2SVP) are given in parentheses

Compound[a]	δ^1H (P*H*)	$\delta^{31}P$ ($\delta_{calc}{}^{31}P$)	$^1J_{P,H}$ (P*H*)	$\delta^{13}C$ (C≡N)	$^1J_{P,C}$ (C≡N)
4a	5.57 [5.95][b]	−105.4 [−101.6][b] (−139.1)	252.3 [249.7][b]	120.8 [121.2][b]	76.3 [74.4][b]
4b	4.38	−120.6 (−154.9)	244.8	116.7	76.7
4c	4.35	−120.4 (−154.6)	247.2	116.6	75.3
5a	5.61	−99.2 ()	260.0	121.0	106.8
5b	4.61	−115.1	250.9	—	—
5c	5.03	−108.3	256.1	—	—
MeP(H)CN[39]	4.15	−119.9	227.5	119.6	70.9

[a] In C_6D_6 at room temperature; values in ppm (δ) or Hz (J). [b] previously reported NMR data for **4a** was collected in CD_2Cl_2 [values given in brackets].[39]

increases significantly to $^1J_{P,C}$ = 106.8 Hz (*cf.* **4a** $^1J_{P,C}$ = 76.3 Hz). Interestingly, in the IR spectrum the CN stretch is now visible as a weak band at 2265 cm^{-1}. The $^{11}B\{^1H\}$ NMR resonance at −10.3 ppm is consistent with tetra-substituted boron atoms bearing perfluorinated aryl groups (*cf.* [K(18-crown-6)][SCNB(C_6F_5)$_3$]: $\delta(^{11}B\{^1H\})$ = −12.4 ppm).[40] The three C_6F_5 groups are equivalent as verified by the respective ^{19}F NMR spectrum ($\delta(^{19}F\{^1H\}4$ = −133.9 (*meta*), −155.8 (*para*), and −163.4 (*ortho*) ppm; $\Delta(\delta)^{19}F_{m,p}$ = 7.6 Hz), which is in agreement with other nitrilium borates with a heteroatom at the carbon atom of the C≡N triple bond (*cf.* PhSCNB(C_6F_5)$_3$: $\delta(^{19}F\{^1H\})$ = −134.0 (*meta*), −155.7 (*para*), and −163.3 (*ortho*) ppm; $\Delta(\delta)^{19}F_{m,p}$ = 7.6 Hz).[41] The molecular structure of **5a** (Fig. 4) confirms the four-coordinate boron atom and the BNCP axis is in a nearly linear arrangement (P1–C19–N1 175.7(2)°, C19–N1–B1 178.3(2)°). The N1–C19 bond length of 1.136(3) Å is still diagnostic of a triple bond (*cf.* **4a** 1.143(4) Å; Σr_{cov}(C≡N) = 1.14 Å).[30] The newly formed N1–B1 bond (1.584(3) Å) is in the same range as reported for PhSCNB(C_6F_5)$_3$ (1.5829(10) Å)[41] and slightly shorter when compared to classic nitrile–B(C_6F_5)$_3$ adducts (*cf.* MeCNB(C_6F_5)$_3$ 1.616(3) Å).[42]

Attempted syntheses of cyanophosphides

With **4a–c** in hand, we envisioned to synthesize the corresponding cyanophosphides [RPCN]$^-$ through simple deprotonation of **4a–c**. The first dicyanophosphides [P(CN)$_2$]M were isolated by Schmidtpeter *et al.* through reductive decyanation of P(CN)$_3$,[43] and alternative synthetic strategies have surfaced since this initial report.[44–46] Schmidtpeter and co-workers then

Table 4 Selected bond lengths [Å] and angles [°] of **4a–c** and **5a**

Compound	P–C	N–C	P–C–N	C–P–C
4a	1.796(3)	1.143(4)	176.4(3)	97.49(11)
4b	1.7853(18)	1.148(2)	177.41(16)	100.31(6)
4c	1.793(2)	1.146(3)	177.5(2)	99.32(9)
5a	1.799(3)	1.136(3)	175.7(2)	97.71(11)

synthesized [PhPCN]M (M$^+$ = Na, K, [(Ph$_3$P)$_2$N]) by reacting Ph$_5$P$_5$ with the corresponding cyanides as equilibrium mixtures, which is shifted to [PhPCN]M when using weakly-coordinating cations.[47–49] Recently, Grützmacher *et al.* introduced alkali phosphanyl cyanophospides [(NHP)PCN]M (NHP = N-heterocyclic phosphenium, M = Na, K) as versatile PCN building blocks, by an oxygen for nitrogen exchange from phosphanyl phosphaketenes of the general type (NHP)PCO with (M(NSiMe$_3$)$_2$) (M = alkali metal) and concomitant formation of O(SiMe$_3$)$_2$.[50] Wolf, Weigand and co-workers observed the formation of the phosphanyl-substituted cyanophosphides
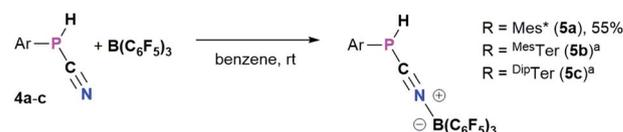
Scheme 4 Synthesis of phosphanitriliumborates ArP(H)CNB(C_6F_5)$_3$ **5a–c**. [a] NMR reactions, products were not isolated.
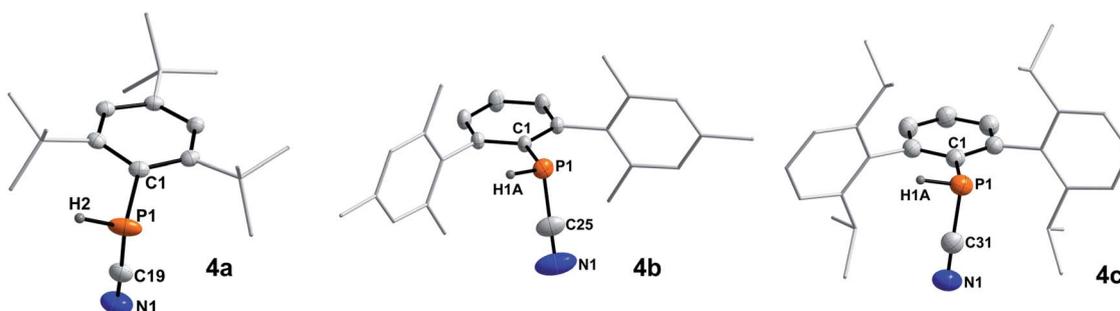

Fig. 3 Molecular structures of **4a** (left), **4b** (middle), and **4c** (right). Hydrogen atoms (except on P1) omitted and parts of the molecules rendered as wireframe for clarity. Thermal ellipsoids are drawn at the 50% probability level. Structural parameters are summarized in Table 4.
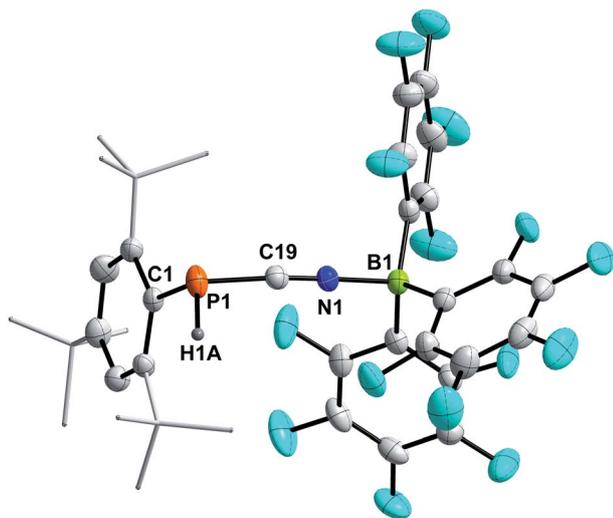
Fig. 4 Molecular structure of 5a. Hydrogen atoms (except H1) omitted and tBu-groups on Mes* rendered as wireframe for clarity. Thermal ellipsoids are drawn at the 50% probability level. Selected bond lengths (Å) and angles (°): P1–C19 1.799(3), N1–C19 1.136(3), N1–B1 1.584(3), P1–C19–N1 175.7(2), C19–N1–B1 178.3(2), C19–P1–C1 97.71(11).

([R$_2$PPCN]$^-$; R = Ph, Cy, tBu, N(iPr)$_2$) as counter-anions for anionic cyclo-triphosphido cobalt complexes.[51] Inspired by these results, the potential of 4a–c being deprotonated by K[N(SiMe$_3$)$_2$] (KHMDS) was investigated (Scheme 5).

As a starting point, the cyanophosphine Mes*P(H)CN (4a) and KHMDS were combined on an NMR scale, accompanied by a color change from colorless to yellow and formation of a colorless precipitate. ^{1}H and ^{31}P{^{1}H} NMR spectra were immediately recorded and show that the main species at this

point showed a ^{31}P{^{1}H} NMR signal at −146.2 ppm, which according to ^{1}H NMR spectroscopy does not bear a P–H function and HN(SiMe$_3$)$_2$ (HMDS, $\delta(^1$H) = 0.10 ppm) was observed as well.[20] This indicated successful deprotonation to give [Mes*PCN]K (6a).

Nevertheless, 6a is unstable at room temperature and after 16 h at room temperature, the ^{31}P{^{1}H} NMR data revealed three signals at 493.2 (Mes*PPMes*, A),[25] −79.7, and −146.2 ppm, respectively.[20] The signal at −79.7 ppm is now the main species and was assigned to the known 3,3-dimethyl-5,7-di-tert-butyl-phosphaindane (B).[52] Unfortunately, up to now all attempts to isolate, crystallize or trap 6a have not been successful and only crystals of A and B could be obtained. From a mechanistic point of view, we assume that deprotonation of 4a by KHMDS leads to the formation of HMDS and 6a, the latter then eliminates KCN to give a reactive phosphinidene intermediate capable of both dimerization to give A and capable of insertion of the phosphinidene fragment into one methyl group of one tert-butyl group of the Mes* substituent to yield B.[52] Burg and Slota noted that the stability of species of the type RPHX is greatly enhanced by the steric profile of the substituent R.[53] Therefore, the terphenyl-based cyanophosphines 4b and 4c were expected to make the anions isolable. The reaction of ^{Mes}TerP(H)CN (4b) and KHMDS resulted in an immediate color change of the reaction mixture from colorless to yellow and precipitation of a colorless solid. Interestingly, the clean formation of ^{Mes}TerPP^{Mes}Ter (C) ($\delta(^{31}$P{^{1}H}) = 492.5 ppm) and HMDS were observed even when the reaction mixture is directly analyzed by NMR spectroscopy after reacting both substrates.[20] To get information whether any other phosphorus containing species can be observed (e.g. intermediate formation of a phosphinidene which dimerizes to C), 4b and 0.5 eq. of KHMDS were
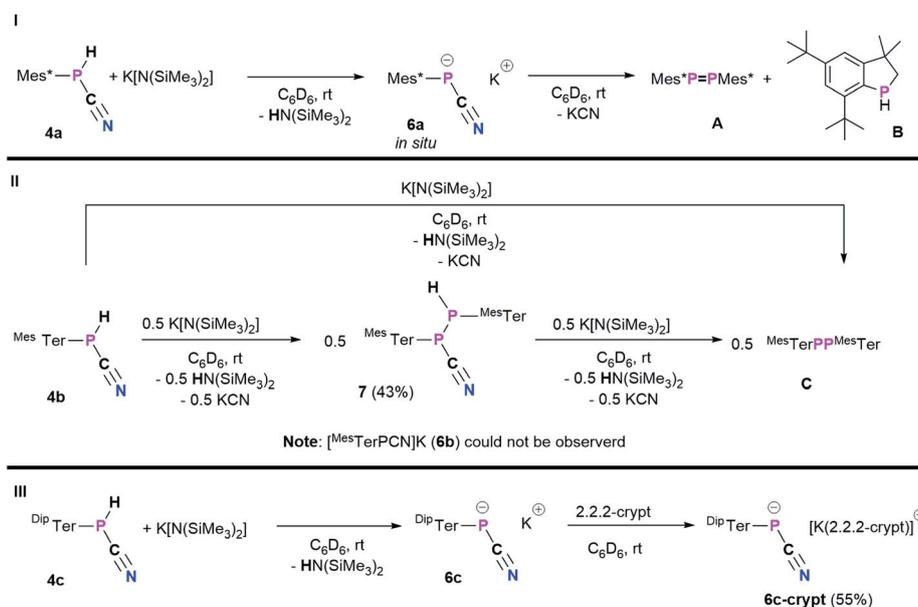
Scheme 5 Reactivity of 4a–c towards KHMDS: (I) in situ synthesis of [Mes*PCN]K (6a) and decomposition towards phosphaindane A, diphosphene B and KCN; (II) synthesis of ^{Mes}TerP(H)P(CN)^{Mes}Ter (7) or diphosphene C dependent on the used stoichiometry; (III) synthesis of [^{Dip}TerPCN]K (6c) and [^{Dip}TerPCN][K(2.2.2-crypt)] (6c-crypt).

combined and the solution was directly analyzed by NMR spectroscopy. Intriguingly, two doublet signals were observed in the $^{31}P\{^1H\}$ NMR spectrum at -78.2 and -82.6 ppm with a coupling constant of $^1J_{P,P} = 326.6$ Hz. The corresponding ^{31}P NMR spectrum revealed the existence of two doublets of doublets with additional coupling constants of 38.3 Hz and 216.3 Hz, respectively. In addition, a highly diagnostic doublet of doublet signal in the ^1H NMR spectrum at 3.97 ppm confirms that the above mentioned coupling constants correspond to $^1J_{P,H}$ and $^2J_{P,H}$ coupling, thus the obtained molecule bears a unique P(H)–P moiety.[20] In accordance with the NMR data and high-resolution mass spectrometry, SC-XRD verified the formation of the diphosphane $^{Mes}TerP(H)P(CN)^{Mes}Ter$ (7, Fig. S1†). Treatment of 7 with additional amounts of KHMDS then resulted in the clean conversion to give diphosphene C as shown by $^{31}P\{^1H\}$ NMR spectroscopy. It is worth mentioning, that the reaction of 4a with half an equivalent of KHMDS only leads to the described concomitant formation of 6a, A, B, KCN, and HMDS with parts of 4a remaining unreacted. Finally, the even bulkier cyanophosphine $^{Dip}TerP(H)CN$ (4c) was reacted with equimolar amounts of KHMDS, giving an immediate color change to yellow. A significantly shielded signal in the $^{31}P\{^1H\}$ NMR spectrum at -142.0 ppm (c.f. in situ prepared 6a: $\delta(^{31}P\{^1H\}) = -146.2$ ppm; [(NHP)PCN]M: $\delta(^{31}P\{^1H\}) = -124$ to -84 ppm[50]) indicated the formation of the corresponding cyanophosphide [$^{Dip}TerPCN$]K (6c). 6c proved to be stable in C_6D_6 solution for at least one week at room temperature. Subsequently, the potassium cation could be sequestered by adding 2.2.2-cryptand to quantitatively give the ion separated salt [$^{Dip}TerPCN$][K(2.2.2-crypt)] (6c-crypt). The ion separation leads to the expected low-field shift in the $^{31}P\{^1H\}$ NMR of approximately 20 ppm so that a signal at -120.7 ppm is detected. In addition, the molecular structure of 6c-crypt was determined by SC-XRD (Fig. 5).

The structural parameters of the $P^{(-)}CN$ unit indicate that the negative charge is mainly located at the phosphorus, with a N1–C31 bond length of 1.1585(19) Å ($\Sigma r_{cov}(C\equiv N) = 1.14$ Å,[30] cf. $Ph_3PC(H)CN$ 1.158(3) Å).[54] This is minimally longer than in starting material 4a (1.146(3) Å), whereas the P1–C31 bond length is slightly shortened (1.7680(14) Å; c.f. 4a: 1.793(2) Å). Therefore a major contribution from the resonance structure R–$P^{(-)}$–C≡N and a minor contribution from the resonance structure R–P=C=N$^{(-)}$ is reasonable, and is further supported by the C–N stretching frequency of 2053 cm^{-1}. The only other structurally characterized cyanophosphides bear phosphorus based substituents at the phosphorus atom of the PCN moiety but show nearly identical bond lengths across the PCN axis (c.f. [iPr$_2$PPCN]$^-$: P–C 1.763(1) Å, N–C 1.160(2) Å;[51] [(NHP)PCN]$^-$: P–C$_{avg}$. 1.75 Å, N–C$_{avg}$ 1.16 Å).[50] Whereas for the previously described cyanophosphides nearly linear arrangements of the PCN moieties are observed (N–C–P > 177°),[50,51] the P1–C31–N1 bond angle of 165.45(12)° deviates significantly from linearity which might be caused by steric repulsion of the sterically demanding ^{Dip}Ter group.

Reactivity of selected 1,3-phosphaazaallenes towards B(C$_6$F$_5$)$_3$ and Pier's borane HB(C$_6$F$_5$)$_2$

Heteroallenes like carbodiimides, isocyanates, and isothiocyanates have shown a diverse reactivity towards the perfluorinated boranes B(C$_6$F$_5$)$_3$ and HB(C$_6$F$_5$)$_2$ (Pier's borane), ranging from the development of new heterocycles to the formation of classic and frustrated Lewis pairs (FLPs) and 1,2-hydroboration reactions.[41,55–58]

Treatment of 3a with B(C$_6$F$_5$)$_3$ in toluene afforded a colorless suspension (Scheme 6, top). After stirring for 16 h and subsequent workup,[20] the isolated colorless solid was hardly soluble in aromatic hydrocarbons and started to polymerize tetrahydrofuran within minutes. From a saturated C_6D_6 solution sufficient ^1H, $^{11}B\{^1H\}$, $^{19}F\{^1H\}$, and $^{31}P\{^1H\}$ data was obtained and the $^{31}P\{^1H\}$ NMR spectrum showed two characteristic signals at -46.8 and -53.3 ppm, respectively with a characteristic $^1J_{P,P} = 247.5$ Hz coupling constant, reminiscent of $^{Mes}TerP(H)P(CN)^{Mes}Ter$ (7) (c.f. $\delta(^{31}P\{^1H\}) = -78.2$ and -82.6 ppm, $^1J_{P,P} = 326.6$ Hz). The existence of a P(H)–P moiety was supported by the ^1H and ^{31}P NMR data, which show that the signal at -53.3 ppm is a doublet of doublets with $^1J_{P,H} = 224.0$ Hz, which is further corroborated by a doublet signal with the same $^1J_{P,H}$ coupling constant in the ^1H NMR spectrum at 5.44 ppm. The reaction is accompanied by significant amounts of
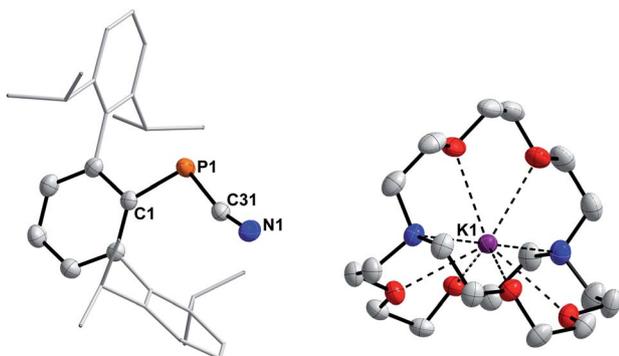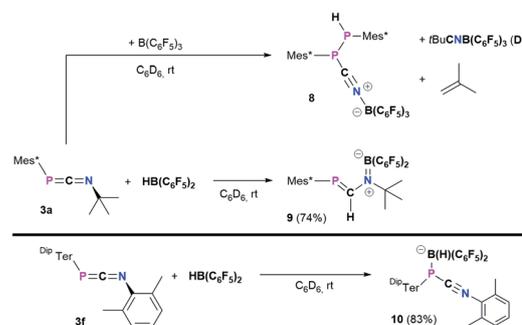

Fig. 5 Molecular structure of 6c-crypt. Hydrogen atoms omitted and Dip-groups rendered as wireframe for clarity. Thermal ellipsoids are drawn at the 50% probability level. Selected bond lengths (Å) and angles (°): P1–C31 1.7680(14), N1–C31 1.1585(19), P1–C31–N1 165.45(12), C1–P1–C31 106.73(6).

Scheme 6 Reactivity of 3a towards B(C$_6$F$_5$)$_3$ and HB(C$_6$F$_5$)$_2$, and reactivity of 3f towards HB(C$_6$F$_5$)$_2$ to give 10.

byproducts as evident from two signals in the $^{11}B\{^1H\}$ NMR spectrum at −7.9 (significantly broadened) and −20.7 ppm, respectively. Similarly, the $^{19}F\{^1H\}$ NMR spectrum shows a total of nine signals. Moreover, iso-butene was identified as byproduct ($\delta(^1H)$ = 1.60 and 4.74 ppm, Fig. S67†), similarly to the synthesis of the cyanophosphines **4a–c**.

Crystallization attempts gave two types of colorless crystals, and SC-XRD confirmed that indeed the diphosphane Mes*P(H) P(CNB(C_6F_5)$_3$)Mes* (**8**, Fig. 6) was formed alongside the literature known nitrile–borane adduct tBuCNB(C_6F_5)$_3$ (**D**) (Scheme 6, top).[42] It is worth mentioning, that all attempts to isolate **8** in pure fashion failed up to now, which is attributed to quite similar solubilities of **8** and **D**. In **8** the newly formed P1–P2 and N1–B1 bond lengths of 2.2464(8) Å and 1.572(3) Å are in good accordance with the formulation as single bonds ($\Sigma r_{cov}(P–P)$ = 2.22 Å; $\Sigma r_{cov}(N–B)$ = 1.56 Å).[30] The N1–C37 bond length of 1.140(3) Å is a typical carbon nitrogen triple bond ($\Sigma r_{cov}(C\equiv N)$ = 1.14 Å),[30] and the P1,C37,N1,B1 axis is minimally bent (e.g. C37–N1–B1 174.9(2)°).

All these metrics agree with phosphanitrilium borate **5a** (Fig. 4). It is noteworthy that the phosphaketene [sP]PCO reacted with B(C_6F_5)$_3$ to give a zwitterionic diphosphirenium with a P_2C three-membered ring with an exocyclic C–O–B(C_6F5)$_3$ moiety.[21] We continued to investigate the reactivity of **3a** towards Pier's borane (HB(C_6F_5)$_2$) to check its potential for hydroboration chemistry.[59]

The reaction of **3a** and HB(C_6F_5)$_2$ yielded a yellow solid after workup (isolated yield 74%, Scheme 6, middle). Single crystals grown from layering a saturated C_6D_6 solution with n-hexane revealed the product to be Mes*PC(H)N(tBu)B(C_6F_5)$_2$ (**9**, Fig. 7), showing that 1,2-hydroboration across the C=N bond of **3a** had occurred (Scheme 6, middle). Remarkably, the molecular structure of **9** reveals a novel heterodiene (P=C–N$^{(+)}$=B$^{(−)}$) structural motif. Both, the P1–C19 and N1–B1 bond lengths of

Fig. 6 Molecular structure of **8**. Hydrogen atoms (except H1) omitted and tBu-groups on Mes* rendered as wireframe for clarity. Thermal ellipsoids are drawn at the 50% probability level. Selected bond lengths (Å) and angles (°): P1–P2 2.2464(8), N1–B1 1.572(3), P1–C37 1.784(2), P1–C1 1.844(2), P2–C19 1.852(2), N1–C37 1.140(3); P1–C37–N1 165.4(2), C37–N1–B1 174.9(2).
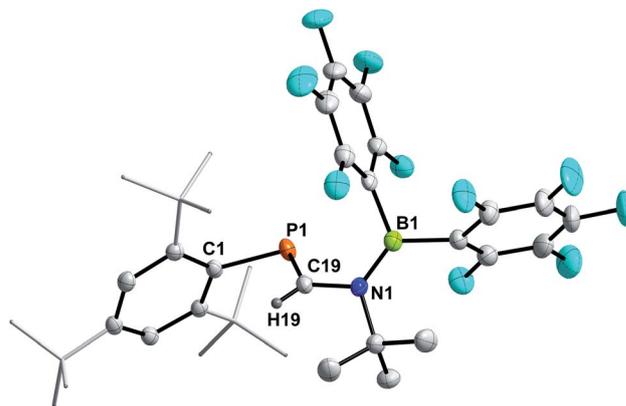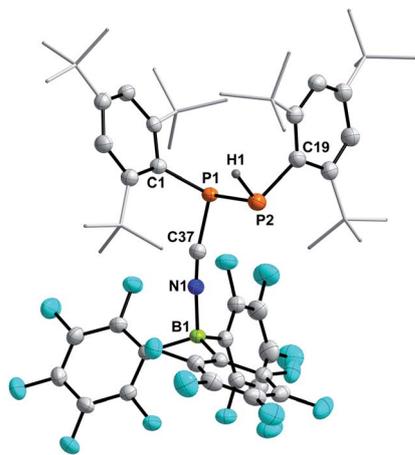

Fig. 7 Molecular structure of **9**. Hydrogen (except H19) omitted and tBu-groups on Mes* rendered as wireframe for clarity. Thermal ellipsoids are drawn at the 50% probability level. Selected bond lengths (Å) and angles (°): P1–C19 1.6751(13), N1–C19 1.4278(15), N1–B1 1.3995(18); C1–P1–C19 98.93(6), P1–C19–N1 123.69(9), C19–N1–B1 120.15(10).

1.6751(13) Å and 1.3995(18) Å are best described as double bonds, respectively, which is also illustrated in the KS orbitals (PBE0-D3/def2-SVP, Fig. S91†). The HOMO is best described as the P–C and B–N π-bonds, respectively, with one node. The LUMO has π* character for P–C and B–N bonds resulting in two nodes and with π-character between C and N, as expected for a heterodiene.[60] The nature of BN multiple bonds has been in the focus of recent computational studies,[61,62] and NBO results for **9** show a σ (N 79.5, B 20.5%) and π (N 86.1, B 13.9%) NBO, which are mainly formed by the natural atomic hybrid orbitals located on N. This agrees well with the values obtained for 9,10-diimino-9,10-dihydro-9,10-diboraanthracene.[62,63] Topological analysis of the electron density using the QT-AIM approach revealed an electron density ($\rho_{(3,−1)}$ [e bohr$^{−3}$]) of 0.198 at the BN bond critical point (BCP), as well as an electron density Laplacian (∇^2 [e bohr$^{−5}$]) of 0.651, which corresponds nicely with the aforementioned diminodiboraanthracene.[20,62] In addition, the sum of angles around C19, N1, and B1 all add up to over 359.8°, in line with sp^2-hybridization. The solution NMR spectra of **9** are indicative that this diene structure sustains in solution, with one resonance in the ^{11}B NMR spectrum at 36.4 ppm, indicating a tri-coordinated boron atom (cf. (C_6F_5)$_2$BNMe$_2$ 33.7 ppm).[64] Given the double bond character of the B=N bond, two distinct C_6F_5 groups are detected giving two sets of signals in the ^{19}F NMR spectrum. Highly diagnostic is the ^1H NMR chemical shift of the P=C(H) proton at 7.80 ppm as a doublet with a $^2J_{P,H}$ coupling constant of 18.5 Hz (cf. Mes*P=C(H) N(SiMe$_3$)$_2$ (ref. 65) $\delta(^1H)$ = 8.24 (d, $^2J_{P,H}$ = 16.8 Hz)). The aforementioned ^1H NMR signal, the deshielded $^{31}P\{^1H\}$ NMR signal at 228.5 ppm and the $^{13}C\{^1H\}$ NMR signal of the P=C(H) functionality ($\delta^{13}C\{^1H\}$ = 177.5 ppm, $^1J_{P,C}$ = 37.3 Hz) clearly indicate a phosphaalkene (cf. 2,6-(Mes*P=C(H))$_2$(NC$_5$H$_5$) $\delta(^{31}P)$ = 249.1 ppm).[66] Interestingly, carbodiimides react with Pier's Borane to the corresponding four-membered boron amidinates.[55] Similar four-membered heterocycles are formed when isothiocyanates are treated with HB(C_6F_5)$_2$.[41]
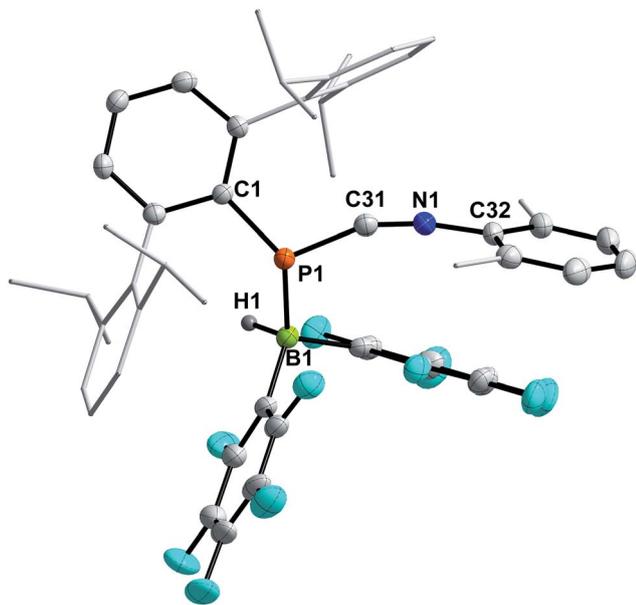
Fig. 8 Molecular structure of **10**. Hydrogen (except H1) omitted and Dip and Xyl groups rendered as wireframe for clarity. Thermal ellipsoids are drawn at the 50% probability level. Selected bond lengths (Å) and angles (°): P1–C31 1.754(3), N1–C31 1.161(3), P1–B1 2.060(3); P1–C31–N1 157.7(2).

Finally, the influence of the substitution pattern at both the phosphorus and nitrogen atoms was investigated exemplarily by reacting the 1,3-phosphaazaallene **3f** (bearing ^{Dip}Ter and Xyl substituents) with $HB(C_6F_5)_2$ (Scheme 6, bottom). One singlet signal in the $^{11}B\{^1H\}$ NMR spectrum at −19.3 ppm, indicated a four-coordinate boron atom. In contrast to **9**, only three signals are observed in the $^{19}F\{^1H\}$ NMR spectrum and the $^{31}P\{^1H\}$ signal is observed at −83.1 ppm, over 300 ppm shifted towards higher field when compared to **9**. These data together with the data obtained by SC-XRD showed that instead of 1,2-hydroboration, the Lewis acid base adduct ^{Dip}TerP(HB(C$_6$F$_5$)$_2$) CNXyl (**10**) with a newly formed P–B bond was obtained (Fig. 8). The C1–N1 bond length of 1.161(3) Å is shortened by approximately 0.04 Å when compared to the starting material **3f** (c.f. 1.2009(15) Å) and is now close to a carbon nitrogen triple bond ($\Sigma r_{cov}(C\equiv N) = 1.14$ Å).[25] Accordingly, the C31–N1–C32 bond angle increases to 165.1(3)° (c.f. 143.24(12)° (**3f**)). The P1–C31 bond length of 1.754(3) Å also increases compared to **3f** (1.6785(12) Å) indicative of a single bond (c.f. ^{Dip}TerP(H)CN **4c** 1.793(2) Å). The P1–B1 bond length of 2.060(3) Å is 0.1 Å longer than the respective sum of the covalent radii ($\Sigma r_{cov}(P–B) = 1.96$ Å)[25] and corresponds with dative bonding as further ascertained by a low WBI for the P–B bond of 0.85.

Conclusions

Phospha-Wittig reagents have been shown to react with isocyanides to give 1,3-phosphaazaallenes **3a–f**. In case of the CNtBu-derivatives these were further transformed in the corresponding cyanophosphines **4a–c**. CNtBu acts in this case as a disguised HCN transfer reagent. This allowed the structural

characterization of this underrepresented class of phosphines and deprotonation yielded in one case a rare example of an aryl-substituted cyanophosphide anion. Moreover, **3a** was shown to be 1,2-hydroborylated along the C=N bond to give the unique heterodiene **9** with alternating PC and BN double bonds. Studies using cyanophosphide **6c** as a ligand and exploiting heterodiene **9** in FLP-type chemistry are currently underway.

Data availability

All experimental, crystallographic and computational data are provided in the ESI.

Author contributions

M. F. discovered and optimized the formation of 1,3-phosphaazaallenes, studied the scope and studied the reactivity of compounds **3a–f**. M. F. prepared the experimental part and the first draft of the manuscript. C. H.-J. designed the overall research, supervised the work, carried out the computational work, contributed to IR analysis, finalized the manuscript, proofread the experimental part and coordinated the overall project.

Conflicts of interest

There are no conflicts to declare.

Notes and references

1 O. I. Kolodiazhnyi, *Tetrahedron Lett.*, 1982, **23**, 4933–4936.

2 O. I. Kolodiazhnyi, *Phosphorus Sulfur Relat. Elem.*, 1983, **18**, 39–42.

3 M. Yoshifuji, K. Toyota, K. Shibayama and N. Inamoto, *Tetrahedron Lett.*, 1984, **25**, 1809–1812.

4 M. Yoshifuji, T. Niitsu, K. Toyota, N. Inamoto, K. Hirotsu, Y. Odagaki, T. Higuchi and S. Nagase, *Polyhedron*, 1988, **7**, 2213–2216.

5 R. Appel and C. Behnke, *Z. Anorg. Allg. Chem.*, 1987, **555**, 23–35.

6 X.-G. Zhou, L.-B. Zhang, R.-F. Cai, Q.-J. Wu, L.-H. Weng and Z.-E. Huang, *J. Organomet. Chem.*, 2000, **604**, 260–266.

7 C. Wentrup, H. Briehl, G. Becker, G. Uhl, H. J. Wessely, A. Maquestiau and R. Flammang, *J. Am. Chem. Soc.*, 1983, **105**, 7194–7195.

8 M.-A. David, J. B. Alexander, D. S. Glueck, G. P. A. Yap, L. M. Liable-Sands and A. L. Rheingold, *Organometallics*, 1997, **16**, 378–383.

9 T. Wegmann, M. Hafner and M. Regitz, *Chem. Ber.*, 1993, **126**, 2525–2530.

10 J. Grobe, D. Le Van and T. Großpietsch, *Z. Naturforsch. B*, 1991, **46**, 978–984.

11 T. L. Breen and D. W. Stephan, *J. Am. Chem. Soc.*, 1995, **117**, 11914–11921.

12 E. Ionescu, G. von Frantzius, P. G. Jones and R. Streubel, *Organometallics*, 2005, **24**, 2237–2240.

13 F. Basuli, L. A. Watson, J. C. Huffman and D. J. Mindiola, *Dalton Trans.*, 2003, 4228–4229.

14 G. Becker, H. Brombach, S. T. Horner, E. Niecke, W. Schwarz, R. Streubel and E.-U. Würthwein, *Inorg. Chem.*, 2005, **44**, 3080–3086.

15 L. Liu, D. A. Ruiz, D. Munz and G. Bertrand, *Chem*, 2016, **1**, 147–153.

16 P. Willmes, M. J. Cowley, M. Hartmann, M. Zimmer, V. Huch and D. Scheschkewitz, *Angew. Chem., Int. Ed.*, 2014, **53**, 2216–2220.

17 P. Gupta, J.-E. Siewert, T. Wellnitz, M. Fischer, W. Baumann, T. Beweries and C. Hering-Junghans, *Dalton Trans.*, 2021, **50**, 1838–1844.

18 M. Fischer, S. Nees, T. Kupfer, J. T. Goettel, H. Braunschweig and C. Hering-Junghans, *J. Am. Chem. Soc.*, 2021, **143**, 4106–4111.

19 M. Fischer, F. Reiß and C. Hering-Junghans, *Chem. Commun.*, 2021, **57**, 5626–5629.

20 Experimental and computational details, and details on the X-ray diffraction studies are included in the ESI.† CCDC 2086496–2086506 contain the X-Ray data.

21 M. M. Hansmann, D. A. Ruiz, L. L. Liu, R. Jazzar and G. Bertrand, *Chem. Sci.*, 2017, **8**, 3720–3725.

22 M. M. Hansmann and G. Bertrand, *J. Am. Chem. Soc.*, 2016, **138**(49), 15885–15888.

23 J. Escudié, H. Ranaivonjatovo and L. Rigon, *Chem. Rev.*, 2000, **100**, 3639–3696.

24 E. Urnéžius and J. D. Protasiewicz, *Main Group Chem.*, 1996, **1**, 369–372.

25 M. Yoshifuji, I. Shima, N. Inamoto, K. Hirotsu and T. Higuchi, *J. Am. Chem. Soc.*, 1981, **103**, 4587–4589.

26 C. Riplinger and F. Neese, *J. Chem. Phys.*, 2013, **138**, 034106.

27 C. Riplinger, B. Sandhoefer, A. Hansen and F. Neese, *J. Chem. Phys.*, 2013, **139**, 134101.

28 R. C. Smith and J. D. Protasiewicz, *J. Am. Chem. Soc.*, 2004, **126**, 2268–2269.

29 S. Shah, M. C. Simpson, R. C. Smith and J. D. Protasiewicz, *J. Am. Chem. Soc.*, 2001, **123**, 6925–6926.

30 P. Pyykkö and M. Atsumi, *Chem.–Eur. J.*, 2009, **15**, 12770–12779.

31 M. B. Smith and J. March, Localized Chemical Bonding, In *March's Advanced Organic Chemistry*, ed. M. B. Smith and J. March, 2006, pp. 3–31.

32 T. Peddarao, A. Baishya, M. K. Barman, A. Kumar and S. Nembenna, *New J. Chem.*, 2016, **40**, 7627–7636.

33 M. K. Sharma, D. Rottschäfer, S. Blomeyer, B. Neumann, H.-G. Stammler, M. van Gastel, A. Hinz and R. S. Ghadwal, *Chem. Commun.*, 2019, **55**, 10408–10411.

34 K. Takeuchi, M. Ichinohe and A. Sekiguchi, *J. Am. Chem. Soc.*, 2012, **134**, 2954–2957.

35 J. Böhnke, H. Braunschweig, T. Dellermann, W. C. Ewing, T. Kramer, I. Krummenacher and A. Vargas, *Angew. Chem., Int. Ed.*, 2015, **54**, 4469–4473.

36 H. Braunschweig, I. Krummenacher, M.-A. Légaré, A. Matler, K. Radacki and Q. Ye, *J. Am. Chem. Soc.*, 2017, **139**, 1802–1805.

37 R. C. Dobbie, P. D. Gosling and B. P. Straughan, *J. Chem. Soc., Dalton Trans.*, 1975, 2368–2373.

38 C. Schulten, G. von Frantzius, G. Schnakenburg and R. Streubel, *Heteroat. Chem.*, 2011, **22**, 275–286.

39 A. Maraval, A. Igau, C. Lepetit, A. Chrostowska, J.-M. Sotiropoulos, G. Pfister-Guillouzo, B. Donnadieu and J. P. Majoral, *Organometallics*, 2001, **20**, 25–34.

40 I. C. Vei, S. I. Pascu, M. L. H. Green, J. C. Green, R. E. Schilling, G. D. W. Anderson and L. H. Rees, *Dalton Trans.*, 2003, 2550–2557.

41 M. Fischer and M. Schmidtmann, *Chem. Commun.*, 2020, **56**, 6205–6208.

42 H. Jacobsen, H. Berke, S. Döring, G. Kehr, G. Erker, R. Fröhlich and O. Meyer, *Organometallics*, 1999, **18**, 1724–1735.

43 A. Schmidpeter and F. Zwaschka, *Angew. Chem., Int. Ed. Engl.*, 1977, **16**, 704–705.

44 A. Schmidpeter, G. Burget, F. Zwaschka and W. S. Sheldrick, *Z. Anorg. Allg. Chem.*, 1985, **527**, 17–32.

45 A. Schmidpeter, F. Zwaschka and W. S. Sheldrick, *Chem. Ber.*, 1985, **118**, 1078–1085.

46 J. F. Binder, S. C. Kosnik, P. B. J. St Onge and C. L. B. Macdonald, *Chem.–Eur. J.*, 2018, **24**, 14644–14648.

47 A. Schmidpeter, K.-H. Zirzow, G. Burget, G. Huttner and I. Jibril, *Chem. Ber.*, 1984, **117**, 1695–1706.

48 A. Schmidpeter and G. Burget, *Z. Naturforsch. B*, 1985, **40**, 1306–1313.

49 R. M. K. Deng and K. B. Dillon, *J. Chem. Soc., Chem. Commun.*, 1981, 1170–1171.

50 Z. Li, J. E. Borger, F. Müller, J. R. Harmer, C.-Y. Su and H. Grützmacher, *Angew. Chem., Int. Ed.*, 2019, **58**, 11429–11433.

51 C. M. Hoidn, T. M. Maier, K. Trabitsch, J. J. Weigand and R. Wolf, *Angew. Chem., Int. Ed.*, 2019, **58**, 18931–18936.

52 A. H. Cowley, F. Gabbai, R. Schluter and D. Atwood, *J. Am. Chem. Soc.*, 1992, **114**, 3142–3144.

53 A. B. Burg and P. J. Slota, *J. Am. Chem. Soc.*, 1958, **80**, 1107–1109.

54 C. Schwarz, L. T. Scharf, T. Scherpf, J. Weismann and V. H. Gessner, *Chem.–Eur. J.*, 2019, **25**, 2793–2802.

55 M. A. Dureen and D. W. Stephan, *J. Am. Chem. Soc.*, 2010, **132**, 13559–13568.

56 M. H. Holthausen, M. Colussi and D. W. Stephan, *Chem.–Eur. J.*, 2015, **21**, 2193–2199.

57 A. C. McQuilken, Q. M. Dao, A. J. P. Cardenas, J. A. Bertke, S. Grimme and T. H. Warren, *Angew. Chem., Int. Ed.*, 2016, **55**, 14335–14339.

58 M. Mehta and J. M. Goicoechea, *Chem. Commun.*, 2019, **55**, 6918–6921.

59 E. A. Patrick and W. E. Piers, *Chem. Commun.*, 2020, **56**, 841–853.

60 G. Desimoni and G. Tacconi, *Chem. Rev.*, 1975, **75**, 651–692.

61 S. Berski, Z. Latajka and A. J. Gordon, *New J. Chem.*, 2011, **35**, 89–96.

62 G. Mierzwa, A. J. Gordon and S. Berski, *J. Mol. Model.*, 2020, **26**, 136.

63 P. Müller, S. Huck, H. Köppel, H. Pritzkow and W. Siebert, *Z. Naturforsch., B: Chem. Sci.*, 1995, **50**, 1476–1484.

64 D. Winkelhaus, Y. V. Vishnevskiy, R. J. F. Berger, H.-G. Stammler, B. Neumann and N. W. Mitzel, *Z. Anorg. Allg. Chem.*, 2013, **639**, 2086–2095.

65 M. Song, B. Donnadieu, M. Soleilhavoup and G. Bertrand, *Chem.–Asian J.*, 2007, **2**, 904–908.

66 Y.-H. Chang, Y. Nakajima and F. Ozawa, *Organometallics*, 2013, **32**, 2210–2215.